Micro-SQUIDs based on MgB2 nano-bridges for NEMS readout

Micro-SQUIDs based on MgB_2 nano-bridges for NEMS readout

2016 Supercond. Sci. Technol. 29 104008

(http://iopscience.iop.org/0953-2048/29/10/104008)

OPEN ACCESS
IOP Publishing
Superconductor Science and Technology
Supercond. Sci. Technol. **29** (2016) 104008 (6pp)
doi:10.1088/0953-2048/29/10/104008

Micro-SQUIDs based on MgB_2 nano-bridges for NEMS readout

L Lolli[1], T Li[2], C Portesi[1], E Taralli[1], N Acharya[3], K Chen[3], M Rajteri[1], D Cox[4], E Monticone[1], J Gallop[2] and L Hao[2]

[1] INRiM, Istituto Nazionale di Ricerca Metrologica, Strada delle Cacce 91, I-10135 Torino, Italy
[2] NPL, National Physical Laboratory, Hampton Rd., Teddington TW11 0LW, UK
[3] Department of Physics, Temple University, Philadelphia Pennsylvania (PA), USA
[4] University of Surrey, Advanced Technology Institute, Guildford, Surrey GU2 7XH, UK

E-mail: l.lolli@inrim.it

Received 30 May 2016, revised 5 August 2016
Accepted for publication 9 August 2016
Published 15 September 2016

Abstract

We show the results obtained from the fabrication and characterisation of MgB_2 loops with two nano-bridges as superconducting weak links. These ring structures are made to operate as superconducting quantum interference devices and are investigated as readout system for cryogenics NEMS resonators. The nano-constrictions are fabricated by EBL and ion beam milling. The SQUIDs are characterised at different temperatures and measurements of the noise levels have been performed. The devices show high critical current densities and voltage modulations under applied magnetic field, close to the critical temperatures.

Keywords: SQUID, magnesium diboride, nano-bridges, NEMS

(Some figures may appear in colour only in the online journal)

1. Introduction

The relatively high superconducting critical temperature of magnesium diboride ($T_c = 39$ K) and its intermetallic properties makes MgB_2 a suitable material to fabricate superconductor quantum interference device (SQUID) [1]. For more than a decade, MgB_2 SQUIDs have been successfully fabricated and studied by several groups [2–7]. Nowadays, MgB_2-based SQUIDs are developed instruments for practical applications [8] and have been integrated into experimental systems, such as for magnetocardiography [9].

In recent years, a key development in SQUIDs has been the approach towards the nanoscale [10, 11]. Micro- and nano-SQUIDs could be used to measure various physical parameters in quantum metrology down to quantum limit [12]. In this field of study, a novel and very promising metrological application of micro-SQUIDs is to reading out nano-electromechanical system (NEMS) [13]. Because of the sizes of the moving parts of NEMS resonators, it is not practical to use a superconducting flux transformer as read out system at sub-micron level. Furthermore, stray inductances between the primary and secondary coils could reduce the coupling. Whereas, even if having an efficient direct coupling between NEMS resonator and micro-SQUID is critical, due to the shapes and the dimensions, nowadays this is the tendency [11, 13].

The key element of a SQUID is the Josephson junction. Dayem bridge technology applied to MgB_2 thin film provides a useful way to prepare Josephson junctions with a size of only a few tens of nanometres, ideal for micro-SQUID incorporation [14]. The long coherence length and the consequently high critical current density gives the advantage of easy manipulation of the junction barrier [11]. This was already demonstrated in nano-constriction on grained MgB_2 film with stable and reproducible technology [4, 6, 15], thus it is possible to use MgB_2 devices to readout NEMS. This new technology is promising over a wide spread of sectors from nanoscale metrology to many possible sensing applications. The aim is the use of the exquisite sensitivity of a SQUID-based readout that offers high flexibility to sense the displacement of a NEMS device through an inductive coupling

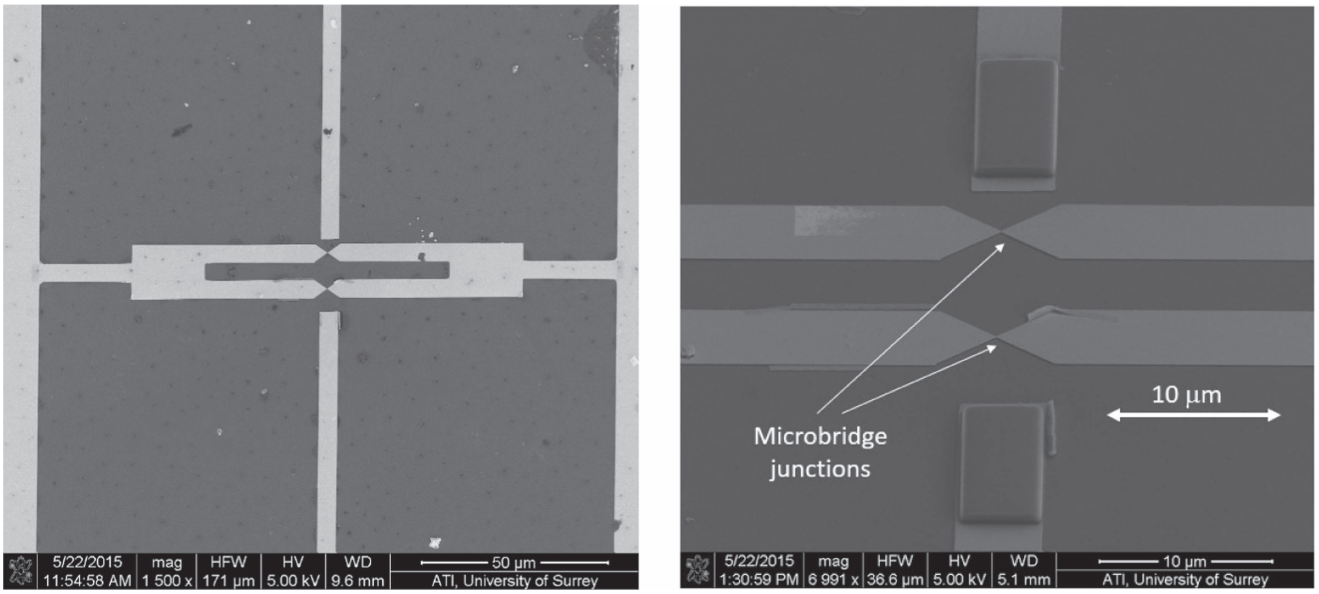

Figure 1. SEM images of the MgB_2 micro-SQUID with leads for NEMS resonator. On the left, an overview of the device D1; on the right, close image of the nano-bridges as Josephson junctions for device D2.

mechanism. The idea behind this work has the purpose of realising magnetometers, which allow optimised coupling between SQUID-readout and NEMS, combined with relatively high operating temperature. In order to reach this goal we fabricated micro-ring structured SQUIDS on very thin epitaxial films, while still maintaining good superconducting properties, and we reduced the constriction dimensions to less than 100 nm, like in [2–7]. The first technique will allow etching by using ion milling instead of focused ion beam, avoiding eventually Ga ion implantation. The second way, moving to nano-constrictions, will permit reduction of the geometric size of the ring-structure.

In this work we present the results of a first step for realising cryogenic SQUID-NEMS combinations. Two magnetometers, based on MgB_2 loop with two nano-constrictions were realised and characterised. The devices were fabricated by an electron beam lithography based approach starting from high quality very thin epitaxial films. Magnetometers properties were measured inside a pulse-tube cryocooler, able to access the temperature range from 2.5 to 40 K.

2. Experimental details

The SQUIDs are based on high quality MgB_2 thin films with thickness of 20 nm, grown by hybrid physical-chemical vapour deposition (HPCVD) on SiC substrates. The HPCVD method has been described in details elsewhere [16] and it allows the fabrication of superconducting magnesium diboride thin films with T_c higher than the bulk value (40 K). In order to protect the superconducting layer from oxidation, a Cr/Au (5 nm/25 nm) layer has been deposited on it.

The coarse structure and the nano-constrictions have been defined by electron beam lithography using MAN2405 negative tone electron resist with a thickness of 500 nm. Then the geometry is transferred from the resist to the film by ion milling of the uncovered superconducting film. The final devices shown in figure 1 are constituted by a SQUID with two additional lateral leads, for subsequent attachment of the SiN microresonator on top of the superconducting loop. On the same MgB_2 thin film were fabricated two SQUIDs called D1 and D2. Figure 1 shows the two magnetometer loops with internal dimension of $65 \times 5\ \mu m^2$; at the centre of the loop there are the two nano-constrictions. D1 and D2 have nano-bridges of 63 nm wide and 55 nm wide, respectively (figure 2).

The SQUIDs have been characterised in a cryocooler with base temperature of 2.5 K. A pancake coil, of NbTi superconducting wire, fixed below the samples, allowed a magnetic field to be applied, so that the voltage modulation can be measured.

3. Results and discussion

Figure 3 shows the resistance versus temperature of the ring structures D1 and D2 measured with an excitation current of 5 μA. Both devices have a two-step transition: a step at higher temperature, close to the film T_c, due to SQUID arms and a step at lower temperature related to constrictions. Similar behaviour have been often observed after nano-structuration of MgB_2 film [6, 17]. The normal state resistance of device D1 is 17.5 Ω and the normal state resistance of device D2 is 27.5 Ω.

In figure 4, typical examples of the measured SQUID current–voltage characteristics are shown for the two samples at several temperatures close to their respective T_c.

Figure 5 depicts the dependence on temperature of the measured critical current (I_c). The experimental data of I_c was very well fitted by the formula [18] $I_c(T) = I_{c0}(1 - T/T_c)^{\alpha}$,

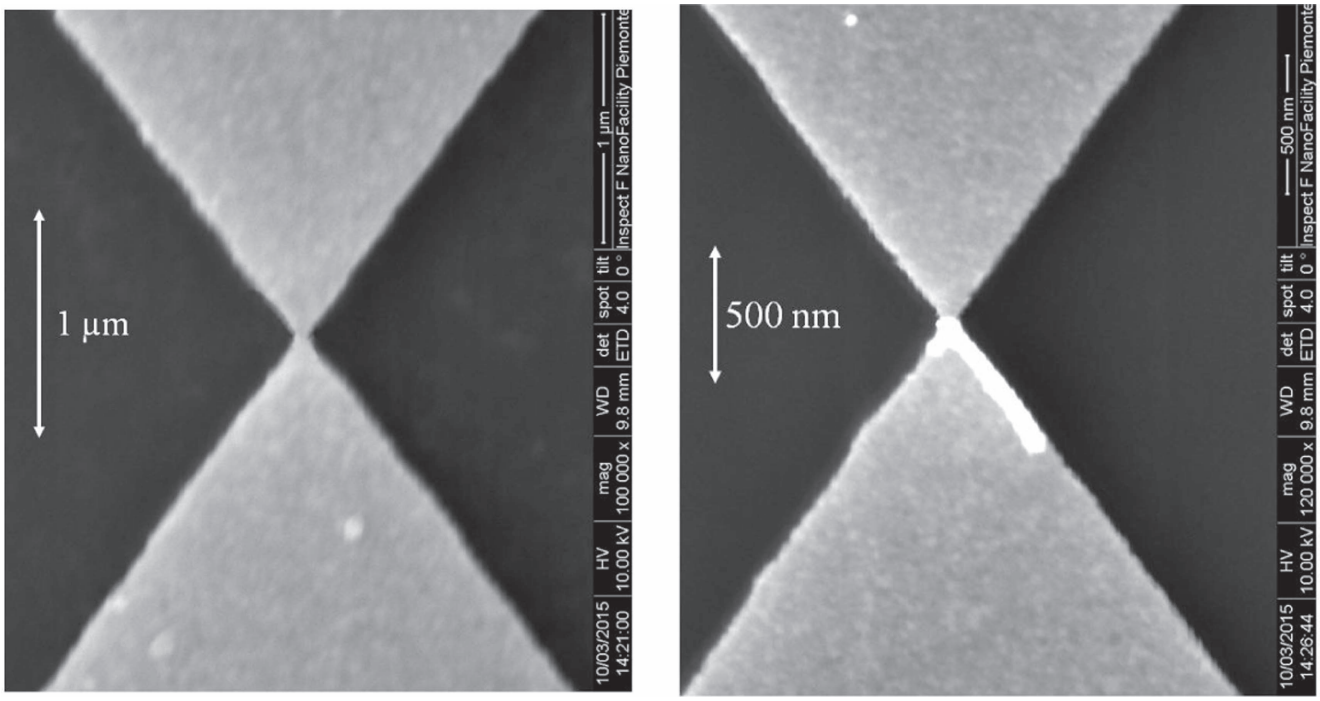

Figure 2. SEM images of the MgB_2 nano-constrictions. On the left, the nano-bridge (D1) is 63 nm wide. On the right, the nano-bridge (D2) is 55 nm wide.

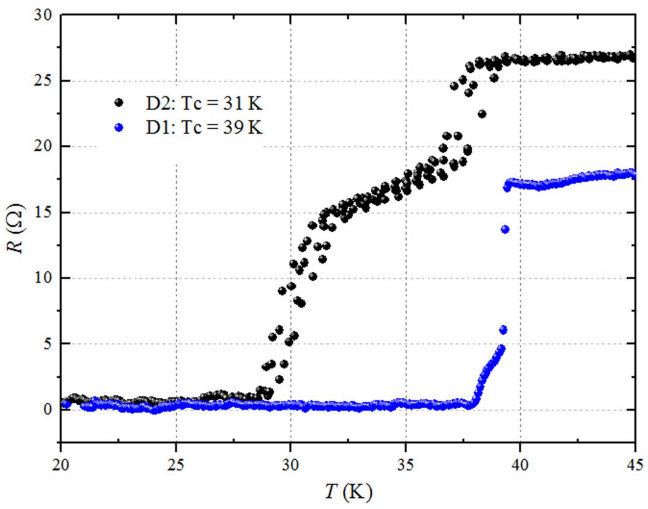

Figure 3. Critical temperatures of the two SQUIDs, measured by the four wire technique.

with α in the range between $1 \div 1.5$ for nano-bridges and between $2 \div 2.5$ for wide bridge. Taking I_{c0}, T_c and α as free parameters in the fit procedure, we obtain critical temperature values close to those estimated by the four-wire technique, which indicates the goodness of the procedure. Whereas, α equals to 1.8 for D1 and 1.3 for D2 leads to behaviours similar to that of long nano-bridges with flux-flow-type [18] and of short nano-bridges based on high quality films [4].

By supposing these $I_c(T)$ behaviours still remain the same also down to lower temperatures, as measured in reference [19], it is possible to estimate the critical current of samples at 4.2 K, by extrapolating from the fits of I_c versus T.

For the D1 device, $I_c(4.2\,\mathrm{K}) \approx 12.2\,\mathrm{mA}$ and, with a bridge cross section estimation of $A = 1.26 \times 10^{-11}\,\mathrm{cm}^2$, the critical current density results $J_c \approx 4.8 \times 10^8\,\mathrm{A\,cm}^{-2}$. Similarly for D2, with $I_c(4.2\,\mathrm{K}) \approx 0.8\,\mathrm{mA}$ and $A = 1.1 \times 10^{-11}\,\mathrm{cm}^2$, we calculate $J_c \approx 3.5 \times 10^7\,\mathrm{A\,cm}^{-2}$. The J_c value of D2 sample results comparable to one obtained in references [4, 5], whereas the D1 device shows a higher current density value, like that reported in [20].

To observe the voltage modulation of the SQUID, the ring structure was biased at constant DC current above the critical current, while the voltage across the ring was monitored as a function of the applied magnetic field. Voltage modulation of the D1 sample has been observed up to 37 K. Figure 6 (left) shows modulations obtained at 36.5 K, biasing D1 SQUID in the range between 42.5 and 55 μA, where the largest modulation amplitude is about 3 μV, at 50 μA.

The effective SQUID area is estimated by the formula $A_{\mathrm{eff}} = \Phi_0/B_{\mathrm{ext}}$, where $\Phi_0 = 2.07 \times 10^{-15}\,\mathrm{T\,m}^2$ and $B_{\mathrm{ext}} = 7.742 \times 10^{-6}\,\mathrm{T}$ is the applied magnetic field needed to have one period of the voltage modulation. With these values, the effective D1 SQUID area result is $2.7 \times 10^{-10}\,\mathrm{m}^2$ (table 1). From the SEM image shown in figure 1, we estimate for the SQUID loop a length of 60 μm and a width of 4.5 μm, from wich the loop geometry area is about $2.98 \times 10^{-10}\,\mathrm{m}^2$. This value is very close to our measured effective area value, any difference probably arising from flux focusing effects due to the relatively wide SQUID loop track. We have measured the voltage as a function of magnetic field at different temperatures, in order to calculate the SQUID effective area as a function of the temperature T, as summarised in table 1. The results indicate that the SQUID effective area is essentially independent of temperature up to 37 K.

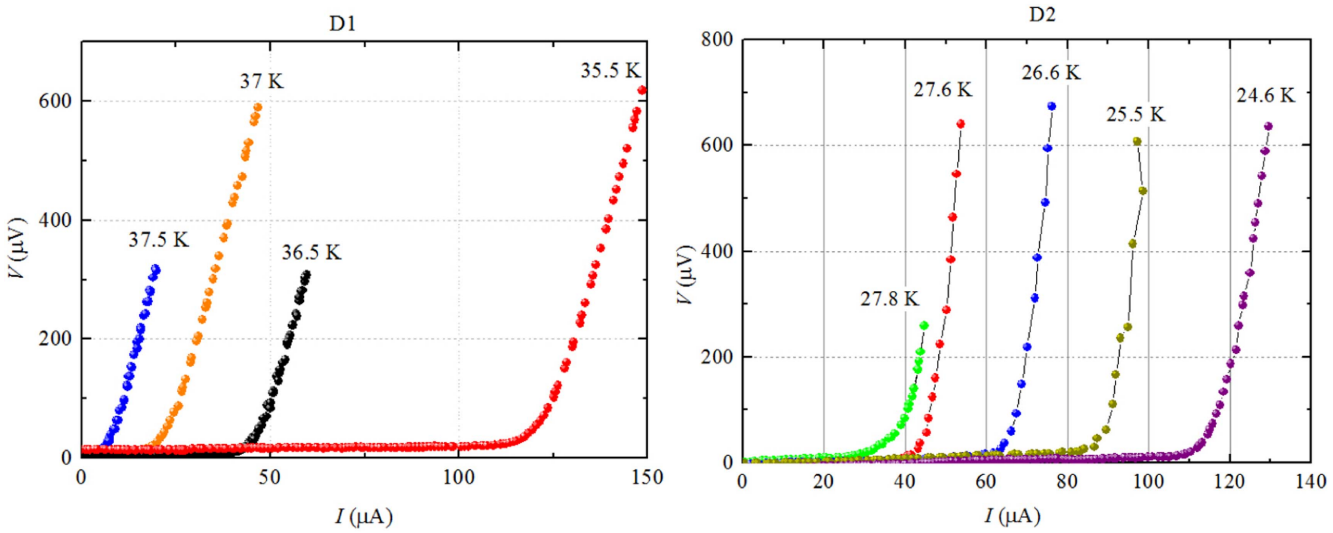

Figure 4. Current–Voltage characteristics of SQUID D1 (left) and D2 (right) in the range 35.5 K–37.5 K and 24.6 K–27.8 K, respectively.

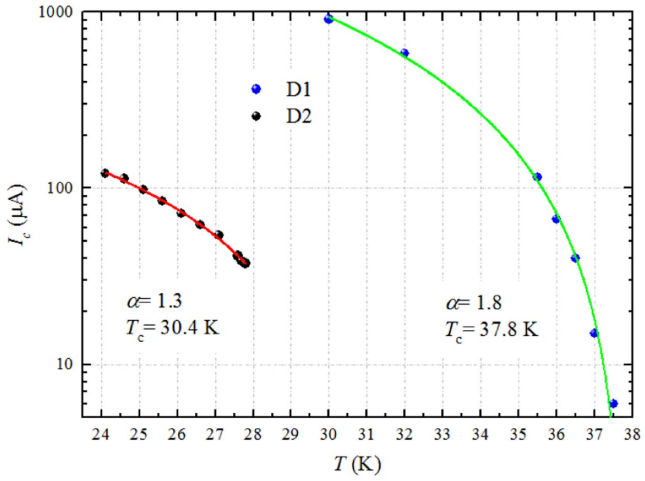

Figure 5. Critical currents of the D1 and D2 SQUID as a function of temperature (dots). The continuous lines show the theoretical fits.

As shown in figure 6 the amplitude of voltage modulation, (the peak-to-peak voltage V_{p-p}) depends on the bias current at a given temperature. Therefore, at a fixed temperature, we have measured some V–Φ curve at different bias current values, and calculated V_{p-p} for each V–Φ plot. Among them, the largest V_{p-p} value for this temperature has been selected (figure 6 right). By repeating this at different temperatures, the trend of V_{p-p} as a function of temperature has been plotted in figure 7, showing that V_{p-p} increases from 0.5 to 7 μV as the temperature changes from 37.5 to 30 K.

The noise spectrum of device D1 was determined under a bias current where the voltage modulation was maximum. A Stanford Research SR 560 voltage amplifier was used to amplify the SQUID output before recording the real-time voltage data and Fourier transforming it. A white noise level of 4.5 nV $Hz^{-1/2}$ is measured and below 10 Hz the noise magnitude is dominated by $1/f$ noise. At an operating temperature of 36.5 K we measured the flux to voltage transfer function $dV/d\Phi = 1.50 \times 10^{-5}$ V/ Φ_0. Using the voltage white noise figure given above for the amplifier we can convert the white flux noise of this device to be 2.7×10^{-4} Φ_0 $Hz^{-1/2}$, a promising figure for such a high operating temperature, given the amplifier limitations. We believe the noise level across the frequency range above 10 Hz is dominated by the room temperature amplifier.

To improve on this we would need to increase the V_{p-p} values in future work, either by making smaller junctions with higher resistance or by making sure the junction properties are matched. Another possibility is to use a low temperature amplifier such as SQUID Series Array Amplifier to improve the MgB_2 SQUID noise performance in future.

4. Conclusions

It is important for future SQUID-NEMS applications that the operating temperature of these combined exquisitely sensitive measurement devices should be at as high a temperature as is practical, in order to simplify operation and reduce complexity. MgB_2 ring structures have been investigated as new SQUID readout for NEMS technologies. With respect to previous MgB_2 devices [2, 3, 6–8], these superconducting micro-rings with Dayem nano-bridges have been fabricated on high quality very thin films (down to 20 nm) of epitaxial MgB_2 [4, 5]. The devices geometries were entirely fabricated by an electron beam lithography reducing the nano-bridges in the width range of 50–65 nm. At least one SQUID still shows voltage modulation as a function of the applied magnetic field up to 37 K. At 36.5 K, the voltage modulation was measured and the noise level of 4.5 nV $Hz^{-1/2}$ seems dominated by the room temperature amplifier. A SiN microresonator has been fabricated and will be positioned on top of the SQUID. These devices show also that is possible to further reduce the dimensions of ring structures (loop and constrictions) while still maintaining the SQUID behaviour.

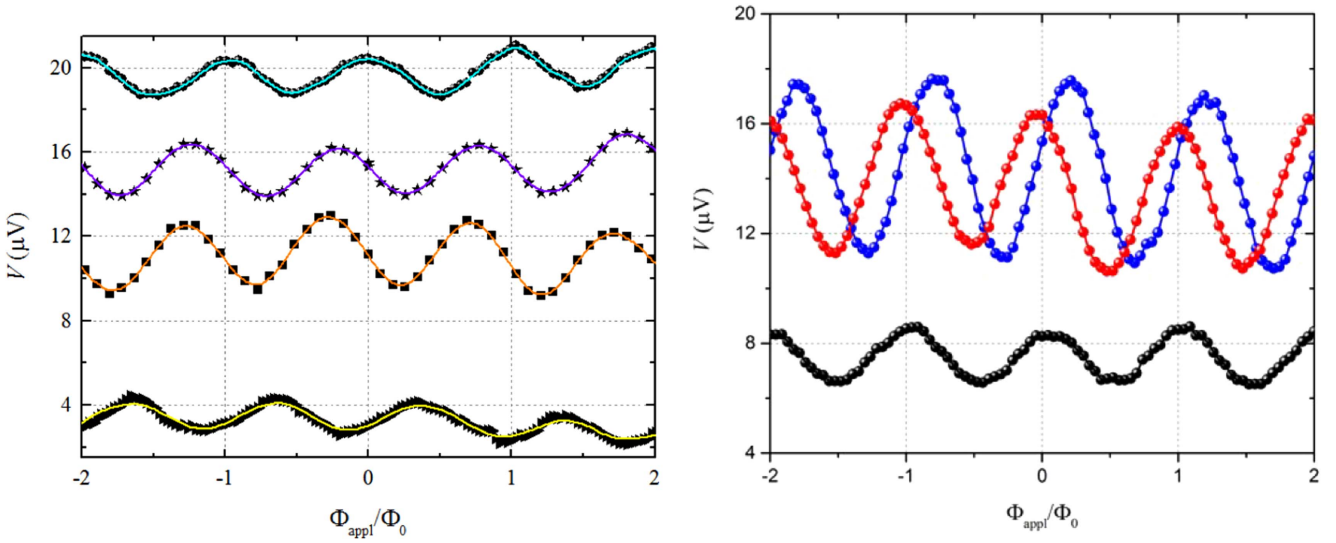

Figure 6. Voltage modulation of SQUID D1 versus applied magnetic field. On the left, at 36.5 K for different values of the bias current ranging between (from the bottom to the top) 42.5, 50, 53 and 55 μA. On the right, the three curves are measured at 37 K (black), 34 K (red) and 31 K (blue) respectively, each of them being with the largest V_{p-p} at given temperature.

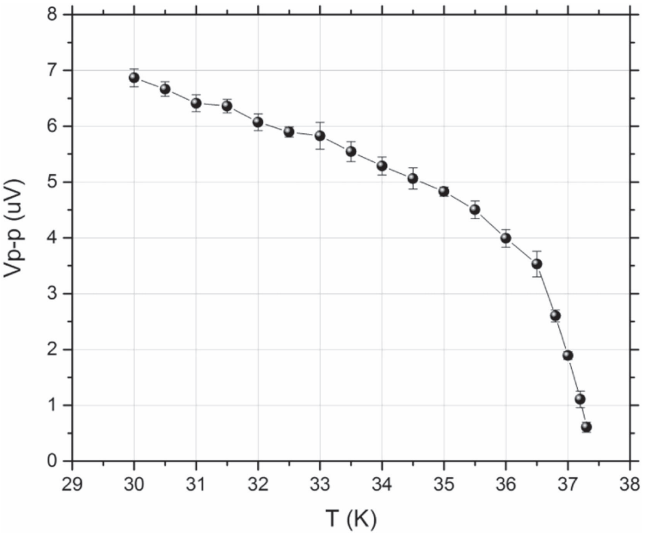

Figure 7. Voltage modulation peak-to-peak value V_{p-p} of SQUID D1 as a function of the temperature.

Table 1. MgB_2 SQUID effective areas versus temperature for device D1.

T(K)	B_{ext} (T)	A_{eff} (m^2)
34.0	7.47×10^{-6}	2.77×10^{-10}
36.5	7.74×10^{-6}	2.67×10^{-10}
37.0	7.50×10^{-6}	2.75×10^{-10}

Acknowledgments

The research within this EURAMET joint research project received funding from the European Community's Seventh Framework Programme, ERA-NET Plus, under Grant Agreement No. 217257. This work was also supported in part by the EMRP (European Metrology Research Programme) project MetNEMS NEW-08 [21] and NMS, UK and in part by 'Nanotechnologies for electromagnetic metrology' program of INRiM, Italy. The EMRP is jointly funded by the participating countries within EURAMET and the European Union.

References

[1] Brinkman A, Veldhuis D, Mijatovic D, Rijnders G, Blank D H A, Hilgenkamp H and Rogalla H 2001 *Appl. Phys. Lett.* **79** 2420–2
[2] Zhang Y, Kinion D, Chen J, Clarke J, Hinks D G and Crabtree G W 2001 *Appl. Phys. Lett.* **79** 3995–7
[3] Burnell G, Kang D J, Ansell D A, Lee H N, Moon S H, Tarte E J and Blamire M G 2002 *Appl. Phys. Lett.* **81** 102–4
[4] Mijatovic D, Brinkman A, Veldhuis D, Hilgenkamp H, Rogalla H, Rijnders G and Blank D H A 2005 *Appl. Phys. Lett.* **87** 192505
[5] Portesi C, Mijatovic D, Veldhuis D, Brinkman A, Monticone E and Gonnelli R S 2006 *Supercond. Sci. Technol.* **19** S303–6
[6] Lee S H, Hong S H, Sung-Hak H, Seong W K and Kang W N 2009 *Supercond. Sci. Technol.* **22** 064009
[7] Lee S H, Hong S H, Kang W N and Kim D H 2009 *J. Appl. Phys.* **105** 013924
[8] Cunnane D, Galan E and Xi X X 2013 *Appl. Phys. Lett.* **103** 212603
[9] Harada Y, Kobayashi K and Yoshizawa M 2012 MgB_2 SQUID for magnetocardiography *Superconductors—Properties, Technology, and Applications* ed Y Grigorashvili (Rijeka: InTech Europe), ISBN: 978-953-51-0545-9
[10] Foley C P and Hilgenkamp H 2009 *Supercond. Sci. Technol.* **22** 064001
[11] Granata C and Vettoliere A 2016 *Phys. Rep.* **614** 1–69
[12] Gallop J C 2003 *Supercond. Sci. Technol.* **16** 1575–82
[13] Hao L, Cox D C, Gallop J C, Chen J, Rozhko S, Blois A and Romans E 2013 *IEEE Trans. Appl. Supercond.* **23** 1800304

[14] Hao L, Gallop J C, Cox D C and Chen J 2015 *IEEE J. Sel. Top. Quantum Electron.* **21** 9100108
[15] Hong S H, Lee S H, Seong W K and Kang W N 2010 *Physica* C **470** S1036–7
[16] Zeng X H *et al* 2002 *Nat. Mater.* **1** 35
[17] Malisa A, Valkeapaa M, Johansson L G and Ivanov Z 2004 *Physica* C **405** 84–8
[18] Schneider J, Kohlstedt H and Wordenweber R 1993 *Appl. Phys. Lett.* **63** 2426
[19] Zhuang C, Chen K, Redwing J M, Li Q and Xi X X 2010 *Supercond. Sci. Technol.* **23** 055004
[20] Chen Y, Yang C, Jia C, Feng Q and Gan Z 2016 *Physica* C **525–526** 56–60
[21] http://metnems.org